 CMES, vol.6, no.3, pp.277-294, 2004

Lie Group Symmetry Applied to the Computation of Convex Plasticity Constitutive Equation

C.-S. Liu[1,2] **and C.-W. Chang**[1]

Abstract: This paper delivers several new types of representations of the convex plasticity equation and realizes them by numerical discretizations. In terms of the Gaussian unit vector and the Weingarten map techniques in differential geometry, we prove that the plastic equation exhibits a Lie group symmetry. We convert the nonlinear constitutive equations to a quasilinear equations system $\dot{\mathbf{X}} = \mathbf{A}\mathbf{X}$, $\mathbf{X} \in \mathbb{M}^{n+1}$, $\mathbf{A} \in so(n,1)$ in local. In this way the inherent symmetry of the constitutive model of convex plasticity is brought out. The underlying structure is found to be a cone in the Minkowski space $\mathbb{M}^{n+1}$ on which the proper orthochronous Lorentz group $SO_o(n,1)$ left acts. Based on the group properties some numerical methods are developed, which together with a post-projecting method can update the stress points on the yield surface at every time increment.

keyword: Computational plasticity, convex plasticity, Lorentz group, consistent scheme.

1 Introduction and model specification

The study of plastic behavior of solid materials under complicated mechanical environment is a very important topic for engineering science and industrial practice, and computational plasticity is a mature subject. In this study a substantial role has been played by the constitutive relations of elastoplasticity, to which many theoretical and experimental contributions and applications have been made; see, e.g., Chen, Yuan and Wittmann (2002), and Sainsot, Jacq and N'elias (2002).

The engineering problems encountered are usually in three dimensions where various stress components interact to cause yielding and plasticity of the material. A yield function includes the effects of all stress components acting in a system to predict the yielding of material. For a general three-dimensional case we have six independent stress components.

The material is said to be in the elastic state if the yield function f is less than 1,

$$f(\mathbf{Q}) < 1, \tag{1}$$

while plastic state if f is exactly equal to 1,

$$f(\mathbf{Q}) = 1, \tag{2}$$

in which $\mathbf{Q}$ denotes the stress vector,

$$\mathbf{Q} := \left[\begin{array}{cccccc} \sigma^{11} & \sigma^{22} & \sigma^{33} & \sigma^{23} & \sigma^{13} & \sigma^{12} \end{array} \right]^{\mathrm{T}}. \tag{3}$$

Throughout this paper a superscript T denotes the transpose. In this paper we focus on the complex problem of convex plasticity and restrict ourselves to a small strain plasticity and thus makes no distinction between the Cauchy stress σ and the Kirchhoff stress τ as that used in the finite strain plasticity by Atluri (1984, 1986), Im and Atluri (1987) and Wang and Atluri (1994).

Many types of the yield functions exist for different materials. For metals, the Tresca, the von-Mises and the Hill yield functions are widely used. For concrete or other geomaterials, the Mohr-Coulomb and the Drucker-Prager yield functions are widely used; see, e.g., Liu (2004a).

Upon combined the two stress states specified in Eqs. (1) and (2), the stress admissible region is

$$f(\mathbf{Q}) \leq 1. \tag{4}$$

Thus, f can never be greater than 1. We are concerned only with the stress-strain relations of perfectly plastic materials. For many practical applications, a material may be idealized and assumed to have a neglible strain-hardening effect. Thus, the above yield function is assumed to be hardening independent; however, it may depend on some material constants.

[1] Department of Mechanical and Mechatronic Engineering, Taiwan Ocean University, Keelung, Taiwan.
[2] Corresponding author. E-mail: csliu@mail.ntou.edu.tw

Corresponding to the stress vector in Eq. (3) there is a conjugate strain vector

$$\mathbf{q} := \left[\begin{array}{cccccc} \varepsilon_{11} & \varepsilon_{22} & \varepsilon_{33} & \varepsilon_{23} & \varepsilon_{13} & \varepsilon_{12} \end{array} \right]^{\mathrm{T}}. \tag{5}$$

We suppose that its rate can be further decomposed additively by

$$\dot{\mathbf{q}} = \dot{\mathbf{q}}^e + \dot{\mathbf{q}}^p, \tag{6}$$

where a superimposed dot denotes the time derivative, and the superscript e surmounted on $\mathbf{q}$ indicates that $\mathbf{q}^e$ is the elastic part of strain deformation, while the plastic strain deformation is denoted by $\mathbf{q}^p$. The physical motivation of the decomposition (6) is the splitting of the stress power $\mathbf{Q}\cdot\dot{\mathbf{q}} = \mathbf{Q}\cdot\dot{\mathbf{q}}^e + \mathbf{Q}\cdot\dot{\mathbf{q}}^p$ into a recoverable part and a dissipative part. Throughout this paper a dot between two vectors stands for their inner product. The above equation is applicable in the range of small strain which can be derived either from a multiplicative decomposition [e.g., Lee and Liu (1967), and Lee (1969)], or as a general postulate [e.g., Nemat-Nasser (1979)]. The legitimacy of Eq. (6) has been discussed by Lee (1981), Nemat-Nasser (1982) and Xiao, Bruhns and Meyers (1999).

As long as the stress state is inside the elastic region, we can use a linearly hypoelastic rule to predict the deformation of the material,

$$\dot{\mathbf{Q}} = k_e\dot{\mathbf{q}}^e, \tag{7}$$

where k_e is an elastic modulus of the material. In the first few sections we consider k_e to be a scalar, and then in Section 8 we extend the computational results to the convex plasticity model endowing with an anisotropic elastic law:

$$\dot{\mathbf{Q}} = \mathbf{K}\dot{\mathbf{q}}^e, \tag{8}$$

where $\mathbf{K}$ is a Voigit matrix form of the fouth-order elastic tensor, which is supposed to be symmetric and positive.

When attempting to cover the deformation with finite strain, Eq. (6) needs to be modified by an additive decomposition of the rate of deformation into an elastic part and a plastic part, while the stress rate in Eqs. (7) and (8) is replaced by a proper corotational stress rate. Mandel (1971) has supplemented the multiplicative decomposition of the deformation gradient into an elastic part and a plastic part proposed by Lee and Liu (1967) with the notion of directors attached to the material substructure in the relaxed configuration. Then Mandel defined a proper corotational rate as the one associated with the spin of the triad of the directors. The extension of Mandel's theory to mixed hardening with internal time has been discussed by Atluri (1986) and Im and Atluri (1987). The material models with different objective stress rates have been studied by Atluri (1984) and some numerical results about the simple shear behaviors were shown there and further clarified by Liu (2004b) with the Lie group integrating methods. Since our aim is to present a clear theory about the convex plasticity, we focus on the convexity of the yield function in the current stage and therefore would pay no attention to the finite strain theory even it is a very important issue in the development of plasticity theory.

According to a plastic irreversibility argument made on elastic-perfectly plastic material [e.g., Chen and Han (1988)], the requirement of positive plastic work leads to convexity of the yield surface and normality of the plastic flow. Thus we assume[3]

$$\dot{\mathbf{q}}^p = \dot{q}_0\mathbf{n}, \tag{9}$$

where

$$\dot{q}_0 \geq 0 \tag{10}$$

is a plastic multiplier, and

$$\mathbf{n} := \frac{\nabla f(\mathbf{Q})}{\|\nabla f(\mathbf{Q})\|} \tag{11}$$

is a unit normal vector standing on the yield surface at a point $\mathbf{Q}$. Here, $\nabla f(\mathbf{Q}) := \partial f(\mathbf{Q})/\partial\mathbf{Q}$, and according to the convexity of yield function we assume that the Hessian matrix associated with f is positive definite, i.e.,

$$\mathbf{H}(\mathbf{Q}) := \nabla^2 f(\mathbf{Q}) > \mathbf{0}, \tag{12}$$

such that the denominator in Eq. (11) is nowhere zero.

A point $\mathbf{Q}\in\mathbb{R}^6$ such that $\nabla f(\mathbf{Q}) \neq \mathbf{0}$ is called a regular point of f; see, e.g., Thorpe (1979). Here, we call f regular if $\nabla f(\mathbf{Q}) \neq \mathbf{0}$ for every $\mathbf{Q}$ in the considered domain. In differential geometry, e.g. Thorpe (1979), the map defined by Eq. (11) is called the Gauss map, and for this reason we give $\mathbf{n}$ a particular name—the Gaussian unit vector.

[3] The foundation of associativity is a material stability postulate, which could be either Drucker's postulate in stress space, or Ilushin's postulate in strain space.

The product of the two inequalities (4) and (10) leads to

$$f(\mathbf{Q})\dot{q}_0 = \dot{q}_0, \tag{13}$$

which together with the just mentioned two inequalities are usually called the complementary-trio. From the above equation two results follow obviously: in the plastic state, i.e. $\dot{q}_0 > 0$, $f = 1$, and in the elastic state, i.e. $f < 1$, $\dot{q}_0 = 0$. The other situations require a further clarification as to be carried out in Section 2.

For a perfectly plastic material, the stress-strain relation in the uniaxial case is rather simple. However, the general behavior of the material under a complex stress state is not so straightforward, because it involves six stress components and six strain components. The question therefore arises as to how integrating these nonlinear differential equations to investigate the behavior of the material under any combined stress state. The nonlinear problem of plasticity is usually treated by different workers in computational plasticity with various numerical schemes. For example, the tangent stiffness-radial return method [e.g., Krieg and Krieg (1977), and Schreyer, Kulak and Kramer (1979)], the radial return method [e.g., Krieg and Krieg (1977)], the elastic predictor-radial corrector method [e.g., Schreyer, Kulak and Kramer (1979)], the generalized midpoint rule [e.g., Ortiz and Popov (1985)], the closest-point-projection algorithm [e.g., Simo and Taylor (1985)], and also the plastic predictor-elastic corrector method [e.g., Nemat-Nasser (1991)]. In order to enforce the consistency condition at every time step the abovementioned algorithms require some iterative calculations to force the stress point at the end of each time step to converge to the yield surface, which is a main source of numerical errors and of consumption of computational time. On the other hand, highly complex expressions defining the yield surfaces may render any conventional calculation method of the second order derivative (needed for a full backward-Euler integrator) almost intractable. Wang and Atluri (1994) have shown that the explicit algorithm of Nemat-Nasser (1991) is not satisfactory due to the convergence problem when the direction of stress keeps changing, as for the non-proportional loading cases, and then proposed a newly modified algorithm which has no problems in convergence and can give a reasonable solution even for large time steps.

The passage directly from the flow model to a numerical scheme may alter or destroy the underlying structure of the model, resulting in unstable, inefficient, and inaccurate calculations. Previously, Hong and Liu (1997, 1998) have exactly linearized the flow model of perfect elastoplasticity with von Mises yield criterion and obtained the closed-form response formulae for the model subjected to rectilinear strain paths. Then, a group theory of the above perfectly elastoplastic model was also developed by Hong and Liu (2000), and a numerical scheme developed fully utilizing the group properties was shown rather promising. Extensions along this direction were also made by several researchers. Auricchio and Beirão da Veiga (2003), according to the work of Hong and Liu (1999a, 2000), extended the integrating factor idea to a linear hardening von Mises model. After some numerical tests, Auricchio and Beirão da Veiga (2003) showed that their new method has a quadratic error convergence while the radial return method shows a linear error convergence behavior. However, their new method does not guarantee to preserve the consistency condition in the plastic loading process as remarked by Liu (2004c). Mukherjee and Liu (2003) and Liu (2004c) have developed consistent numerical schemes without the need of iterations for isotropic hardening and for mixed-hardening materials, respectively. Liu (2004b) has developed the consistent numerical schemes for some large deformation elastoplastic models by considering the quaternionic formulations, which is a great extension of the work by Hong and Liu (1999b) and Liu (2001).

A better understanding of the internal symmetries of the underlying models is not only important in its own right, but will also be beneficial to computation, and often simplifies the solution considerably; see Liu (2003). The most important invariance of perfectly plastic model is that the stress states should stay on the yield surface, which remain unchanged during the plastic deformation. Once one finds internal symmetry in a model of plasticity, one finds among others the key to satisfying the consistency condition. In this paper we propose to approach the symmetry issue and its application on the computation. We analyze the constitutive model of convex plasticity and attempt to achieve a deeper understanding of its underlying structure; more precisely speaking, we explore the structure of Minkowski space $\mathbb{M}^{n+1}$ and the proper orthochronous Lorentz group $SO_o(n,1)$ inherent in the model in the plastic phase. Here, depending on the number of nonzero stress components in Eq. (3) (and correspondingly nonzero strain components in Eq. (5))

which we consider for a physical problem, for example, the axial tension-compression problem, the biaxial tension-compression-torsion problem, etc., the dimension n may be an integer with $1 \leq n \leq 6$, and no matter which case is we use n to denote the physical problem dimension.

We also investigate the dynamics of plasticity equation from several new aspects. First we deliver a geometrical setting of this equation by viewing it as an affine nonlinear dynamical system on the yield manifold in Section 3. In Section 4 we devote to develop a Minkowskian type representation of the convex plasticity equation, which is required later for the development of yield constraint preserving scheme in Section 5. In order to retain the yield constraint we also derive a modified group preserving numerical method in Section 6 by viewing the plasticity equations as a nonlinear differential equations system in the augmented state space. In Section 7 some numerical examples are presented to compare the deveoped integrating schemes. In Section 8 we extend the numerical solutions to convex plasticity by considering the anisotropic elastic law (8), and some conclusions are made in Section 9.

2 Switch for the mechanism of plasticity

In the study of rate-independent plasticity we are always concerned with paths. By a path we mean a continuous curve whose velocity vectors are piecewise continuous. From Eqs. (9) and (10), it is not difficult to prove that

$$\dot{q}_0 = \|\dot{\mathbf{q}}^p\|, \tag{14}$$

which indicates that q_0 is the arc length of a path in the plastic strain space.

We are going to derive the on-off switching criteria for the mechanism of plasticity. Substituting Eqs. (6) and (9) into Eq. (7) gives

$$\dot{\mathbf{Q}} + k_e \dot{q}_0 \mathbf{n} = k_e \dot{\mathbf{q}}. \tag{15}$$

Taking the inner product of Eq. (15) with ∇f gives

$$\nabla f \cdot \dot{\mathbf{Q}} + k_e \dot{q}_0 \|\nabla f\| = k_e \nabla f \cdot \dot{\mathbf{q}}, \tag{16}$$

which asserts that

$$f = 1 \implies k_e \dot{q}_0 \|\nabla f\| = k_e \nabla f \cdot \dot{\mathbf{q}}. \tag{17}$$

Because of $k_e > 0$, we have

$$f = 1 \implies \{\nabla f \cdot \dot{\mathbf{q}} > 0 \iff \dot{q}_0 > 0\}. \tag{18}$$

Thus we deduce the sufficient condition of the following statement:

$$\{f = 1 \text{ and } \nabla f \cdot \dot{\mathbf{q}} > 0\} \iff \dot{q}_0 > 0. \tag{19}$$

On the other hand, if $\dot{q}_0 > 0$, Eq. (13) assures $f = 1$, which together with Eq. (18) assert the necessary condition of the above statement. In other words, the yield condition $f = 1$ and the straining condition $\nabla f \cdot \dot{\mathbf{q}} > 0$ are sufficient and necessary for plastic irreversibility $\dot{q}_0 > 0$. Considering Eq. (19) together with Eqs. (4), (10), (14) and (17), we obtain the following on-off switching criteria for the mechanism of plasticity:

$$\dot{q}_0 = \mathbf{n} \cdot \dot{\mathbf{q}} > 0 \text{ if } f = 1 \text{ and } \nabla f \cdot \dot{\mathbf{q}} > 0, \tag{20}$$

$$\dot{q}_0 = 0 \text{ if } f < 1 \text{ or } \nabla f \cdot \dot{\mathbf{q}} \leq 0. \tag{21}$$

Based on the criteria and the complementary-trio (4), (10) and (13), there are just two phases: the on phase in which $\dot{q}_0 > 0$ and $f = 1$ and the off phase in which $\dot{q}_0 = 0$ and $f \leq 1$. In the on phase the mechanism of plasticity is on and the model exhibits elastoplastic behavior, which is irreversible, while in the off phase the mechanism of plasticity is off and the model responds elastically and reversibly.

3 Plastic equation on the yield manifold

Eqs. (15), (20) and (21) together yield a two-phase affine nonlinear system:[4]

$$\dot{\mathbf{Q}} = k_e \dot{\mathbf{q}} - k_e \mathbf{n} \cdot \dot{\mathbf{q}} \mathbf{n} \text{ if } f = 1 \text{ and } \nabla f \cdot \dot{\mathbf{q}} > 0, \tag{22}$$

$$\dot{\mathbf{Q}} = k_e \dot{\mathbf{q}} \text{ if } f < 1 \text{ or } \nabla f \cdot \dot{\mathbf{q}} \leq 0, \tag{23}$$

of which the latter is linear and represents an instantaneous response, and the former is a system of highly nonlinear differential equations in the n-dimensional space of $\mathbf{Q} = (Q^1, Q^2, \cdots, Q^n)$.

Because Eq. (23) is simple, in the remainder of this paper we concentrate to study the plastic equation (22).

Let S be an $n-1$-dimensional surface in $\mathbb{R}^n$, for example the yield surface. A vector field $\mathbf{x}$ along a parametrized curve $\alpha : I \mapsto S$ is tangent to S along α if $\mathbf{x}(t) \in S_{\alpha(t)}$ for all $t \in I$. Generally the derivative $\dot{\mathbf{x}}$ is not tangent to S. However, we can obtain a vector field tangent to S by

[4] In control theory a system is said to be an affine nonlinear system if it is linear in the inputs but nonlinear in the state variables.

projecting $\dot{\mathbf{x}}$ orthogonally onto $S_{\alpha(t)}$ for each $t \in I$. In the terminology of differential geometry, e.g. Thorpe (1979), the process of differentiating and then projecting onto the tangent space to S defines a linear operation, which is called covariant differentiation:

$$\mathbf{x}' = \dot{\mathbf{x}} - [\dot{\mathbf{x}} \cdot \mathbf{n}(\alpha(t))]\mathbf{n}(\alpha(t)), \tag{24}$$

where $\mathbf{n}(\alpha(t))$ is an orientation at the point $\alpha(t)$ in S. By utilizing this concept we can prove the following result.

Theorem 1. *The plastic equation (22) in terms of the covariant derivative of* $\mathbf{q}$ *on the yield manifold* $\mathbb{M}$ *can be represented by a more neater form:*

$$\mathbf{Q}' = k_e \mathbf{q}', \tag{25}$$

similar to the elastic equation (23) in the Euclidean space $\mathbb{R}^n$.

Proof. Let $\mathbb{M} := \{\mathbf{Q} | f(\mathbf{Q}) = 1\}$ be a smooth convex yield manifold and let $\mathbf{Q}(t)$ be a parametrized curve in $\mathbb{M}$. The covariant derivative of vector $\mathbf{q}(t)$ is the vector field $\mathbf{q}'$ tangent to $\mathbb{M}$ along the curve defined by

$$\mathbf{q}' = \dot{\mathbf{q}} - \dot{\mathbf{q}} \cdot \mathbf{n}\mathbf{n}, \tag{26}$$

which is schematically shown in Fig. 1. On the other hand we have $\mathbf{Q}' = \dot{\mathbf{Q}}$ since $\dot{\mathbf{Q}}$ is a tangent vector on the yield manifold. Through Eq. (22) and the above equations we get the result in Eq. (25), which indicates an "elastic type" constitutive equation on the yield manifold $\mathbb{M}$.

The dissipative term in Eq. (22) has a number of interesting properties. It is not induced by any Rayleigh dissipation function, but is equal to the negative gradient of the yield function multiplied by a plastic dissipation power. Take a vector $\dot{\mathbf{q}}$ in $\mathbb{R}^n$ and orthogonally decompose it in the standard metric on $\mathbb{R}^n$ into vector component tangent to the yield manifold and vector orthogonal to the manifold as shown in Fig. 1 with the following result:

$$\dot{\mathbf{q}} = [\dot{\mathbf{q}} - \dot{\mathbf{q}} \cdot \mathbf{n}\mathbf{n}] + \dot{\mathbf{q}} \cdot \mathbf{n}\mathbf{n}. \tag{27}$$

The tangent component of $\dot{\mathbf{q}}$ can be obtained by applying the projection operator on it:

$$\dot{\mathbf{q}} - \dot{\mathbf{q}} \cdot \mathbf{n}\mathbf{n} = [\mathbf{I}_n - \mathbf{n} \otimes \mathbf{n}]\dot{\mathbf{q}}, \tag{28}$$

where $\mathbf{I}_n$ is the n-dimensional identity matrix and $\otimes$ is the dyadic (tensor) product of vectors. The projection operator has the property: $[\mathbf{I}_n - \mathbf{n} \otimes \mathbf{n}]^2 = \mathbf{I}_n - \mathbf{n} \otimes \mathbf{n}$, which corresponding to the standard metric $\mathbf{I}_n$ on $\mathbb{R}^n$ is called the dissipative metric on the yield manifold; refer Liu (2000).

4 Formulation in the Minkowski space

From the above discussion it is clear that the Gaussian unit vector $\mathbf{n}$ plays a pivotal role for describing plastic evolution on the yield manifold, and is a dual variable of $\dot{\mathbf{q}}$ contributing on the dissipation rate $\dot{q}_0$ as shown in Eq. (20). Let us consider again the unit n-dimensional orientation vector as that defined by Eq. (11).[5] See Fig. 2 for such a formulation. Because ∇f is a monotonic operator of $\mathbf{Q}$ by the assumption (12), there exists a homeomorphism $\mathbf{F}$ between $\mathbf{Q}$ and $\nabla f = \|\nabla f\|\mathbf{n}$, such that

$$\mathbf{Q} = \mathbf{F}(\nabla f) = \mathbf{F}(\|\nabla f\|\mathbf{n}). \tag{29}$$

In the following a methodology will be developed to embed the pair $(\mathbf{n}, \|\nabla f\|)$ into the Minkowski space, and derive a differential equations system about $(\mathbf{n}, \|\nabla f\|)$. This technique was first developed by Liu (2002) to transform the generalized Hamiltonian system to the nonlinear Lorentzian equations system. The main result is given as follows.

Theorem 2. *For the plastic equation (22) with its* f *a regular and strictly convex function of* $\mathbf{Q}$*, we can obtain a nonlinear Lorentzian system representation as follows*:

$$\dot{\mathbf{X}} = \mathbf{A}\mathbf{X}, \tag{30}$$

where $\mathbf{A} \in so(n,1)$ *is a matrix function of* $\mathbf{X}$*, and* $\mathbf{X}$ *satisfies the cone condition* $\mathbf{X}^T\mathbf{g}\mathbf{X} = 0$.

Proof. Upon letting[6]

$$\mathcal{W} := \frac{\mathbf{H}}{\|\nabla f\|}, \tag{31}$$

and taking the differential of Eq. (11) we obtain

$$\dot{\mathbf{n}} = \mathcal{W}\dot{\mathbf{Q}} - \mathbf{n} \cdot (\mathcal{W}\dot{\mathbf{Q}})\mathbf{n}. \tag{32}$$

Inserting Eq. (22) for $\dot{\mathbf{Q}}$ into the above equation one has

$$\dot{\mathbf{n}} = k_e[\mathcal{W} - \mathbf{n} \otimes (\mathcal{W}\mathbf{n})][\mathbf{I}_n - \mathbf{n} \otimes \mathbf{n}]\dot{\mathbf{q}}. \tag{33}$$

[5] For a nonzero vector it is rather natural to express it as a unit vector multiplied by the vector length. However, without more information about the pair $(\mathbf{n}, \|\nabla f\|)$ it can do nothing.

[6] In differential geometry, e.g. Thorpe (1979), the operator $\mathcal{W} := \mathbf{H}/\|\nabla f\|$ defined by Eq. (31) is called the Weingarten map.

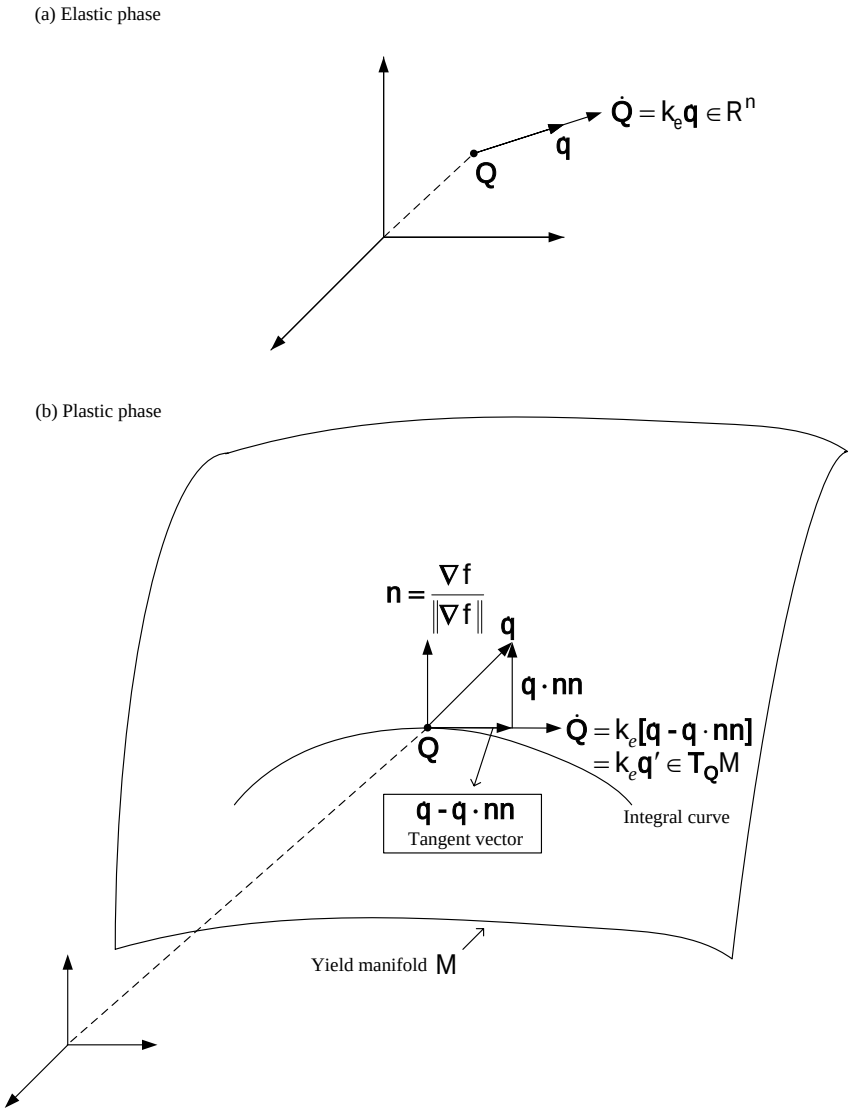

Figure 1 : (a) Elastic phase stress rate-strain rate relation in $\mathbb{R}^n$. (b) Plastic phase stress rate-strain rate relation in $T\mathbb{M}$.

Then, upon defing

$$\mathbf{A}_0^s := k_e[\mathbf{W} - (\mathbf{W}\,\mathbf{n}) \otimes \mathbf{n}]\dot{\mathbf{q}}, \tag{34}$$

from Eq. (33) we have

$$\dot{\mathbf{n}} = \mathbf{A}_0^s - \mathbf{A}_0^s \cdot \mathbf{nn}. \tag{35}$$

Upon considering the integrating factor

$$X^0(t) := \|\nabla f(\mathbf{Q}(t_i))\| \exp\left[\int_{t_i}^{t} (\mathbf{A}_0^s \cdot \mathbf{n}) d\xi\right], \tag{36}$$

where t_i is an initial time, Eq. (35) and the time differential of Eq. (36) become, respectively,

$$\frac{d}{dt}(X^0\mathbf{n}) = X^0\mathbf{A}_0^s, \tag{37}$$

$$\frac{d}{dt}X^0 = X^0\mathbf{A}_0^s \cdot \mathbf{n}. \tag{38}$$

In the homogeneous coordinates

$$\mathbf{X} = \begin{bmatrix} \mathbf{X}^s \\ X^0 \end{bmatrix} = \begin{bmatrix} X^1 \\ \vdots \\ X^n \\ X^0 \end{bmatrix} := X^0 \begin{bmatrix} \mathbf{n} \\ 1 \end{bmatrix}, \tag{39}$$

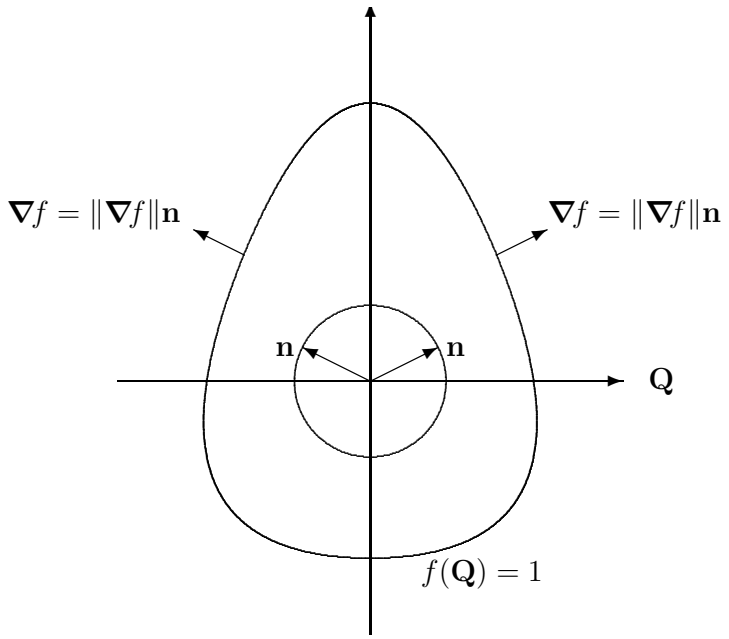

Figure 2 : The gradient of yield function can be expressed as the Gaussian unit vector multiplied by the length of the gradient vector.

Eqs. (37) and (38) together lead to Eq. (30), where

$$\mathbf{A} := \begin{bmatrix} \mathbf{0}_n & \mathbf{A}_0^s \\ (\mathbf{A}_0^s)^{\mathrm{T}} & 0 \end{bmatrix}. \tag{40}$$

It is easy to check that $\mathbf{A}$ satisfies

$$\mathbf{A}^{\mathrm{T}}\mathbf{g} + \mathbf{g}\mathbf{A} = \mathbf{0}, \tag{41}$$

where the Minkowski metric is

$$\mathbf{g} := \begin{bmatrix} \mathbf{I}_n & \mathbf{0}_{n\times 1} \\ \mathbf{0}_{1\times n} & -1 \end{bmatrix}. \tag{42}$$

However, since $\mathbf{A}$ is not only the function of the control input $\dot{\mathbf{q}}$ but also of X^0 and $\mathbf{n}$, it is a local Lie algebra of the proper orthochronous Lorentz group $SO_o(n,1)$, denoted correspondingly by $so(n,1)$, where n and 1 are used to stress that there are n's +1 and one -1 in the metric tensor $\mathbf{g}$ and also signifies the dimensions $n+1$ of the Lie algebra.

Taking the time differential of $\|\nabla f\|$, which with the aid of Eqs. (11) and (12), leads to

$$\frac{d}{dt}\|\nabla f\| = \mathbf{n}\cdot(\mathbf{H}\dot{\mathbf{Q}}). \tag{43}$$

In view of Eq. (22) it becomes

$$\frac{d}{dt}\|\nabla f\| = k_e\mathbf{n}\cdot(\mathbf{H}\dot{\mathbf{q}}) - k_e\mathbf{n}\cdot\dot{\mathbf{q}}\mathbf{n}\cdot(\mathbf{H}\mathbf{n}). \tag{44}$$

Substituting Eq. (34) into Eq. (38) it follows that

$$\frac{\dot{X}^0}{X^0} = k_e\mathbf{n}\cdot(\mathit{W}\,\dot{\mathbf{q}}) - k_e\mathbf{n}\cdot\dot{\mathbf{q}}\mathbf{n}\cdot(\mathit{W}\,\mathbf{n}). \tag{45}$$

Dividing Eq. (44) by $\|\nabla f\|$ and comparing it with the above equation by noting Eq. (31) we obtain

$$\frac{\dot{X}^0}{X^0} = \frac{\frac{d}{dt}\|\nabla f\|}{\|\nabla f\|}. \tag{46}$$

Integrating it and using the initial condition $X^0(t_i) = \|\nabla f(\mathbf{Q}(t_i))\|$ identified from Eq. (36), give us a meaningful formula,

$$X^0 = \|\nabla f\|. \tag{47}$$

From the above equation together with Eqs. (11) and (39) the following identity is verified:

$$\mathbf{X}^s = \nabla f. \tag{48}$$

Thus, we have system (30) with

$$\mathbf{X} = \begin{bmatrix} \mathbf{X}^s \\ X^0 \end{bmatrix} = \begin{bmatrix} \nabla f \\ \|\nabla f\| \end{bmatrix}, \tag{49}$$

and the following $\mathbf{A}_0^s$:

$$\mathbf{A}_0^s = k_e\,\mathit{W}\,\dot{\mathbf{q}} - \frac{k_e}{\|\nabla f\|^2}\nabla f\cdot\dot{\mathbf{q}}\,\mathit{W}\,\nabla f, \tag{50}$$

which is obtained from Eq. (34) by replacing $\mathbf{n}$ by $\nabla f/\|\nabla f\|$; however, $\boldsymbol{W}$ should be viewed as function of ∇f through the homeomorphism (29) between $\mathbf{Q}$ and ∇f.

From the definition (39) it is very natural to endow a *cone* in the Minkowski space,

$$\mathbf{X}^{\mathrm{T}}\mathbf{g}\mathbf{X}=0. \tag{51}$$

Furthermore, in terms of $(\nabla f,\|\nabla f\|)$ through the identification (49), it holds the following condition:

$$\nabla f\cdot\nabla f-\|\nabla f\|^2=\|\nabla f\|^2-\|\nabla f\|^2=0, \tag{52}$$

which is the most natural condition that we can put in the flow model. In Fig. 3 the cone is plotted. The above ends the proof.

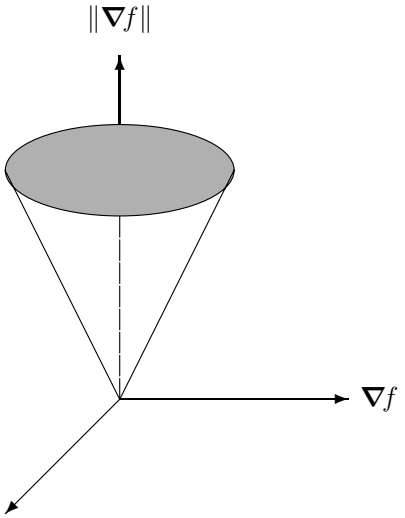

Figure 3 : The construction of cone in the space $(\nabla f,\|\nabla f\|)$ rendering a Minkowskian type representation of convex plasticity possible.

5 Yield constraint preserving scheme–MGPS in space $(\nabla f,\|\nabla f\|)$

The evolutions of elastic equations are rather simple, and we below turn our attention to the numerical solutions of plastic equations. The numerical scheme would provide a medium to calculate the value of $\mathbf{X}$ at time $t=t_{\ell+1}$ when already knowing $\mathbf{X}$ at time $t=t_\ell$. The evolution of $\mathbf{X}$ is governed by the dynamical law (30) with matrix $\mathbf{A}$ given by Eq. (40). Due to the piecewise linearity of controlled strain, $\dot{\mathbf{q}}$ is constant in each time increment equal to Δt. Unluckily, due to the presence of $\mathbf{X}$ in Eq. (50), this is not true for matrix $\mathbf{A}$. Therefore we approximate the solution of the dynamical law (30) considering $\mathbf{X}$ constant in each single time step. Under such an additional hypothesis, the matrix $\mathbf{A}$ is constant, and so the evolution of Eq. (30) is known to be

$$\mathbf{X}(\ell+1)=\mathbf{G}(\ell)\mathbf{X}(\ell), \tag{53}$$

where

$$\begin{aligned}\mathbf{G}(\ell)&:=\exp[\Delta t\mathbf{A}(\ell)]\\&=\begin{bmatrix}\mathbf{I}_n+\frac{z_1(\ell)-1}{\|\mathbf{A}_0^s(\ell)\|^2}\mathbf{A}_0^s(\ell)(\mathbf{A}_0^s)^{\mathrm{T}}(\ell) & \frac{z_2(\ell)}{\|\mathbf{A}_0^s(\ell)\|}\mathbf{A}_0^s(\ell)\\ \frac{z_2(\ell)}{\|\mathbf{A}_0^s(\ell)\|}(\mathbf{A}_0^s)^{\mathrm{T}}(\ell) & z_1(\ell)\end{bmatrix},\end{aligned} \tag{54}$$

in which

$$z_1(\ell):=\cosh(\Delta t\|\mathbf{A}_0^s(\ell)\|),\ \ z_2(\ell):=\sinh(\Delta t\|\mathbf{A}_0^s(\ell)\|). \tag{55}$$

A numerical algorithm is called a *group preserving scheme* (GPS) if for every time increment the map from $\mathbf{X}(\ell)$ to $\mathbf{X}(\ell+1)$ preserves the following group properties:

$$\mathbf{G}^{\mathrm{T}}\mathbf{g}\mathbf{G}=\mathbf{g}, \tag{56}$$

$$\det\mathbf{G}=1, \tag{57}$$

$$G_0^0\geq 1, \tag{58}$$

where G_0^0 is the 00-th component of $\mathbf{G}$ located at the right-lower corner of the matrix as that z_1 is in Eq. (54).

In order to match the consistency condition exactly, we impose the yield condition $f(\mathbf{Q})=1$ on the numerical solutions of $\mathbf{X}(\ell+1)$, which by Eqs. (29) and (47) leads to

$$f(\mathbf{F}(X^0(\ell+1)\mathbf{n}(\ell+1)))-1=0. \tag{59}$$

Here $\mathbf{n}(\ell+1)=\mathbf{X}^s(\ell+1)/X^0(\ell+1)$ is still calculated by scheme (53), and then substituting it into the above equation we obtain a nonlinear algebraic equation to solve a new $X^0(\ell+1)$. This technique is one of the post-projecting methods usually employed to solve differential algebraic equations.

In order to solve Eq. (59) we however need a numerical method, e.g. the half-interval method, to finish this work, and after that we update the old $\mathbf{X}^s(\ell+1)$ to a new

one by $\mathbf{X}^s(\ell+1)=X^0(\ell+1)\mathbf{n}(\ell+1)$ with $X^0(\ell+1)$ just solved. In the later we will show that the consistency error through the above modification becomes very small within a given error tolerance. We call the latter a *modified group preserving scheme* (MGPS), which preserves the internal symmetry $PSO_o(n,1)$ for the unit vector $\mathbf{n}$, and also the yield constraint by enforcing the consistency condition. Its drawback is needing to search the homeomorphism function $\mathbf{F}$.

6 Yield constraint preserving scheme–MGPS in space $(\mathbf{Q},\|\mathbf{Q}\|)$

In this section we develop another scheme to preserve the yield constraint. Let us consider Eq. (22) again, which together with the differential equation for the magnitude of $\mathbf{Q}$ can be rearranged to

$$\frac{d}{dt}\mathbf{Q}=k_e\dot{\mathbf{q}}-k_e\mathbf{n}\cdot\dot{\mathbf{q}}\mathbf{n}, \tag{60}$$

$$\frac{d}{dt}\|\mathbf{Q}\|=\frac{1}{\|\mathbf{Q}\|}[k_e\mathbf{Q}\cdot\dot{\mathbf{q}}-k_e\mathbf{n}\cdot\dot{\mathbf{q}}\mathbf{Q}\cdot\mathbf{n}]. \tag{61}$$

The above technique was first developed by Liu (2001) for general dynamical systems to embed them into an augmented Minkowski space and then derived the group-preserving scheme.

In terms of augmented state variables

$$\mathbf{X}=\left[\begin{array}{c}\mathbf{X}^s\\ X^0\end{array}\right]:=\left[\begin{array}{c}\mathbf{Q}\\ \|\mathbf{Q}\|\end{array}\right], \tag{62}$$

Eqs. (60) and (61) can be combined together to

$$\dot{\mathbf{X}}=\mathbf{A}\mathbf{X}, \tag{63}$$

where

$$\mathbf{A}:=\left[\begin{array}{cc}\mathbf{0}_n & \mathbf{A}_0^s\\ (\mathbf{A}_0^s)^{\mathrm{T}} & 0\end{array}\right]$$
$$=\frac{k_e}{\|\mathbf{Q}\|}\left[\begin{array}{cc}\mathbf{0}_n & \dot{\mathbf{q}}-\mathbf{n}\cdot\dot{\mathbf{q}}\mathbf{n}\\ \dot{\mathbf{q}}^{\mathrm{T}}-\mathbf{n}\cdot\dot{\mathbf{q}}\mathbf{n}^{\mathrm{T}} & 0\end{array}\right]. \tag{64}$$

Applying the group-preserving scheme (GPS) on Eq. (63) as that done in Section 5, we also obtain the numerical scheme as shown in Eqs. (53)-(55). However, in order to retain the constraint exactly we proceed as follows. From Eqs. (53) and (54) it follows a numerical scheme for $\mathbf{m}:=\mathbf{Q}/\|\mathbf{Q}\|$:[7]

$$\mathbf{m}(\ell+1):=\frac{\|\mathbf{A}_0^s(\ell)\|^2\mathbf{m}(\ell)+[(z_1(\ell)-1)\mathbf{A}_0^s(\ell)\cdot\mathbf{m}(\ell)+z_2(\ell)\|\mathbf{A}_0^s(\ell)\|]\mathbf{A}_0^s(\ell)}{z_2(\ell)\|\mathbf{A}_0^s(\ell)\|\mathbf{A}_0^s(\ell)\cdot\mathbf{m}(\ell)+z_1(\ell)\|\mathbf{A}_0^s(\ell)\|^2}. \tag{65}$$

It is easy to check that

$$\|\mathbf{m}(\ell)\|=1\Longrightarrow\|\mathbf{m}(\ell+1)\|=1, \tag{66}$$

which means that scheme (65) preserves the unit length of $\mathbf{m}$. Corresponding to the symmetry $\mathbf{G}\in SO_o(n,1)$, the symmetry preserved by scheme (65) is denoted by $PSO_o(n,1)$, a projection of $SO_o(n,1)$.

In order to match the yield constraint exactly, we impose the yield condition on the numerical solutions, which by $\mathbf{m}=\mathbf{Q}/\|\mathbf{Q}\|=\mathbf{Q}/X^0$ leads to

$$f(X^0(\ell+1)\mathbf{m}(\ell+1))=1, \tag{67}$$

where $\mathbf{m}(\ell+1)$ is already calculated by scheme (65). The above technique is one of the post-projecting methods usually employed to solve differential algebraic equations. However, we extend it to the augmented dynamical system. Due to the convexity of f, Eq. (67) has one and only one solution of X^0. Substituting $\mathbf{m}(\ell+1)$ into the above equation and solving it by the half-interval method we may obtain a new $X^0(\ell+1)$. With the new $X^0(\ell+1)$ we update $\mathbf{X}^s(\ell+1)=\mathbf{Q}(\ell+1)$ to a new $\mathbf{X}^s(\ell+1)=\mathbf{Q}(\ell+1)=X^0(\ell+1)\mathbf{m}(\ell+1)$, such that $\mathbf{A}_0^s$ defined in Eq. (64) can be calculated, and then use scheme (65) to calculate the next $\mathbf{m}$ and Eq. (67) the next X^0. Here we call such a scheme the *modified group-preserving scheme* (MGPS), which preserves the symmetry $PSO_o(n,1)$ for $\mathbf{m}$ as well as retains the yield constraint. Fig. 4 shows the numerical processes by a closed-loop diagram. The schemes in this section are more effective and direct than that in Section 5, because the former ones are directly applied to the unit vector $\mathbf{m}=\mathbf{Q}/\|\mathbf{Q}\|$, and the latter ones are applied to the unit vector $\mathbf{n}=\nabla f/\|\nabla f\|$.

7 Numerical examples

In this section we employ two numerical examples, one with quadratic yield function and the other with cubic yield function, to demonstrate the performance of the above numerical schemes.

[7] Corresponding to the Gaussian unit vector $\mathbf{n}$ defined by Eq. (11), $\mathbf{m}:=\mathbf{Q}/\|\mathbf{Q}\|$ is a stress unit vector.

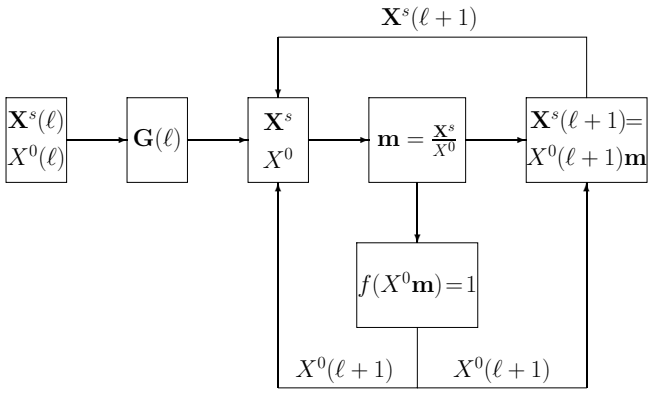

Figure 4 : Instead of the open-loop GPS to calculate $(\mathbf{X}^s(\ell+1), X^0(\ell+1))$ from $(\mathbf{X}^s(\ell), X^0(\ell))$ by left-multiplying them by $\mathbf{G}(\ell)$, in the MGPS we use a closed-loop post-projecting method to enhance the preservation of yield constraint.

7.1 Example one: quadratic yield function

As a first illustrative example let us consider the following quadratic yield function:

$$f = \frac{1}{2}\mathbf{Q}\cdot(\mathbf{HQ}), \tag{68}$$

where $\mathbf{H}$ is an $n\times n$ positive definite matrix of material constants. For this case one has

$$\nabla f = \mathbf{HQ}. \tag{69}$$

Hence, by Eqs. (35), (34) and (44) we obtain

$$\begin{aligned}\frac{d\mathbf{n}}{dt} &= \frac{k_e}{\|\mathbf{HQ}\|}\mathbf{H}\dot{\mathbf{q}} - \frac{k_e\mathbf{n}\cdot\dot{\mathbf{q}}}{\|\mathbf{HQ}\|}\mathbf{Hn} \\ &- \frac{k_e}{\|\mathbf{HQ}\|}\mathbf{n}\cdot(\mathbf{H}\dot{\mathbf{q}})\mathbf{n} \\ &+ \frac{k_e}{\|\mathbf{HQ}\|}\mathbf{n}\cdot\dot{\mathbf{q}}\mathbf{n}\cdot(\mathbf{Hn})\mathbf{n}, \end{aligned}\tag{70}$$

$$\frac{d}{dt}\|\mathbf{HQ}\| = k_e\mathbf{n}\cdot(\mathbf{H}\dot{\mathbf{q}}) - k_e\mathbf{n}\cdot\dot{\mathbf{q}}\mathbf{n}\cdot(\mathbf{Hn}). \tag{71}$$

If ∇f is available, via Eq. (69) the responses are calculated by

$$\mathbf{Q} = \|\mathbf{HQ}\|\mathbf{H}^{-1}\mathbf{n}. \tag{72}$$

For this example $\mathbf{A}_0^s$ is

$$\mathbf{A}_0^s = \frac{k_e}{\|\mathbf{HQ}\|}\mathbf{H}\dot{\mathbf{q}} - \frac{k_e}{\|\mathbf{HQ}\|^3}(\mathbf{HQ})\cdot\dot{\mathbf{q}}\mathbf{H}^2\mathbf{Q}, \tag{73}$$

and thus the equations system reads as

$$\begin{aligned}\frac{d}{dt}\begin{bmatrix}\mathbf{HQ}\\ \|\mathbf{HQ}\|\end{bmatrix} &= \frac{k_e}{\|\mathbf{HQ}\|^3} \\ &\begin{bmatrix}\mathbf{0}_{n\times n} & \|\mathbf{HQ}\|^2\mathbf{H}\dot{\mathbf{q}} - (\mathbf{HQ})\cdot\dot{\mathbf{q}}\mathbf{H}^2\mathbf{Q}\\ \|\mathbf{HQ}\|^2\dot{\mathbf{q}}^{\mathrm{T}}\mathbf{H} - (\mathbf{HQ})\cdot\dot{\mathbf{q}}\mathbf{Q}^{\mathrm{T}}\mathbf{H}^2 & 0\end{bmatrix} \\ &\begin{bmatrix}\mathbf{HQ}\\ \|\mathbf{HQ}\|\end{bmatrix}.\end{aligned}\tag{74}$$

The cone condition obviously reduces to

$$\mathbf{X}^{\mathrm{T}}\mathbf{gX} = (\mathbf{HQ})\cdot(\mathbf{HQ}) - \|\mathbf{HQ}\|^2 = \|\mathbf{HQ}\|^2 - \|\mathbf{HQ}\|^2 = 0.$$

Substituting Eq. (73) into Eq. (54) the group preserving scheme in Section 5 is available for this example.

For simplicity we consider a two-dimensional axial-torsional problem $\mathbf{Q} = (Q^1, Q^2)^{\mathrm{T}}$, for which the yield function becomes

$$\begin{aligned}f &= \frac{1}{2}\mathbf{Q}\cdot(\mathbf{HQ}) \\ &= \frac{1}{2}\left[H_{11}(Q^1)^2 + 2H_{12}Q^1Q^2 + H_{22}(Q^2)^2\right],\end{aligned}\tag{75}$$

where Q^1 is the axial stress and Q^2 the shear stress. The modification (67) of X^0 for this case can be derived exactly and explicitly as follows:

$$X^0(\ell+1) = \sqrt{\frac{2(H_{11}H_{22}-H_{12}^2)}{H_{22}(n^1(\ell+1))^2 - 2H_{12}n^1(\ell+1)n^2(\ell+1) + H_{11}(n^2(\ell+1))^2}}. \tag{76}$$

The following parameters: $H_{11} = 1\times10^{-4}$ 1/MPa^2, $H_{12} = 1.5\times10^{-4}$ 1/MPa^2, $H_{22} = 5\times10^{-4}$ 1/MPa^2, and $k_e = 5\times10^4$ MPa are used on the material model. We first consider a piecewise proportional loading case. Fig. 5 illustrates the responses to an input of a cyclic square path in two dimensions strain space (q_1, q_2) as shown in Fig. 5(a). Substituting Eq. (73) for $\mathbf{A}_0^s$ into the numerical schemes (53) and (54) in Section 5, the responses are calculated. The results include the stress path in Fig. 5(b), hysteresis loops in Figs. 5(c) and 5(d), as well as the errors of consistency condition calculated by GPS and MGPS in Fig. 5(e). It can be seen that the stress paths are located on the yield locus (indicated by dashed line) very well in the plastic phase. The response graph of the stress path in Fig. 5(b) as can be seen is very different

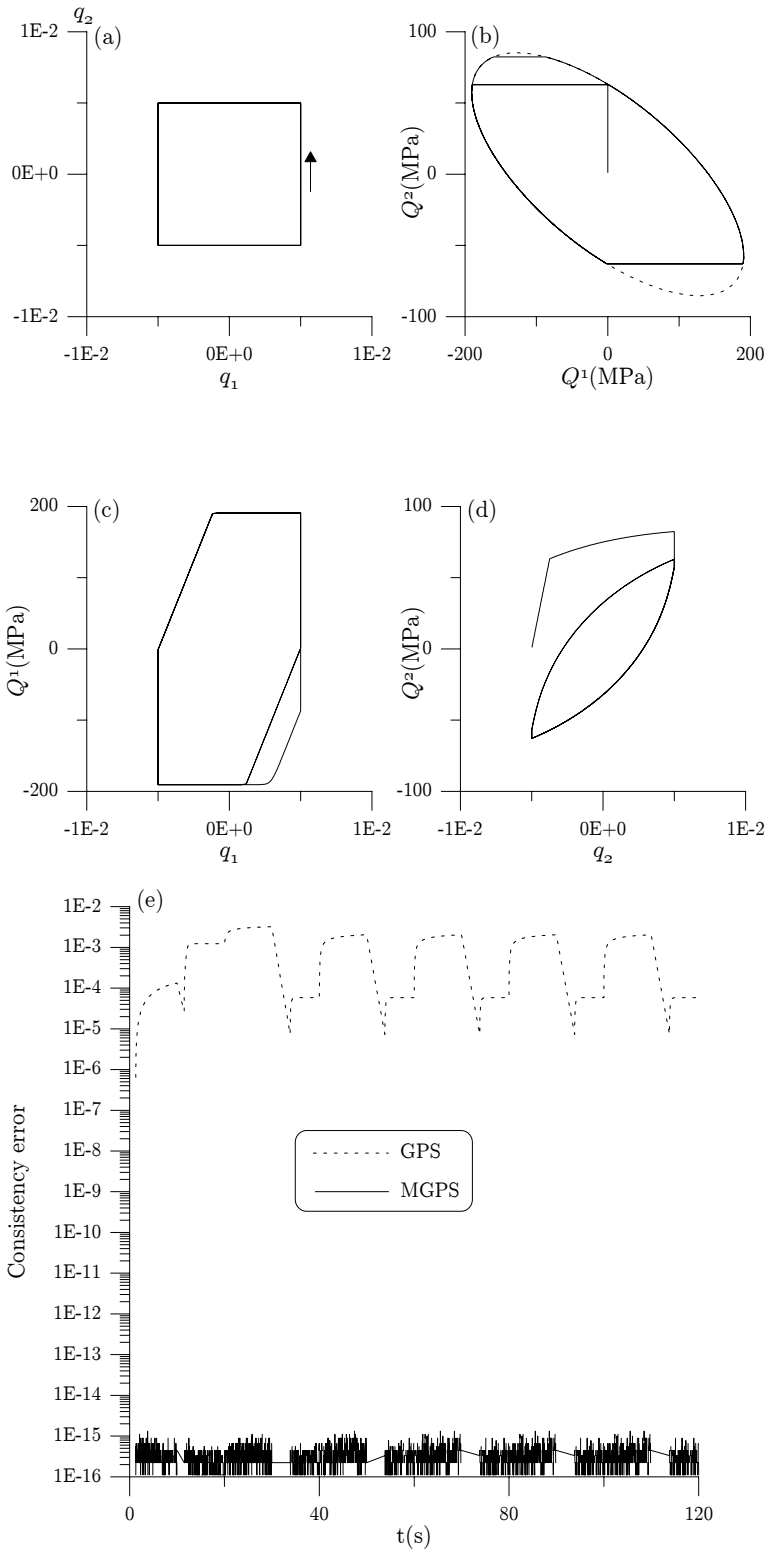

Figure 5 : The responses to a square strain path in (a), and (b) displaying its corresponding stress path, (c) the cyclic axial stress-axial strain curve, (d) the cyclic shear stress-shear strain curve, and (e) errors in satisfying the consistency condition for GPS and MGPS in Section 5.

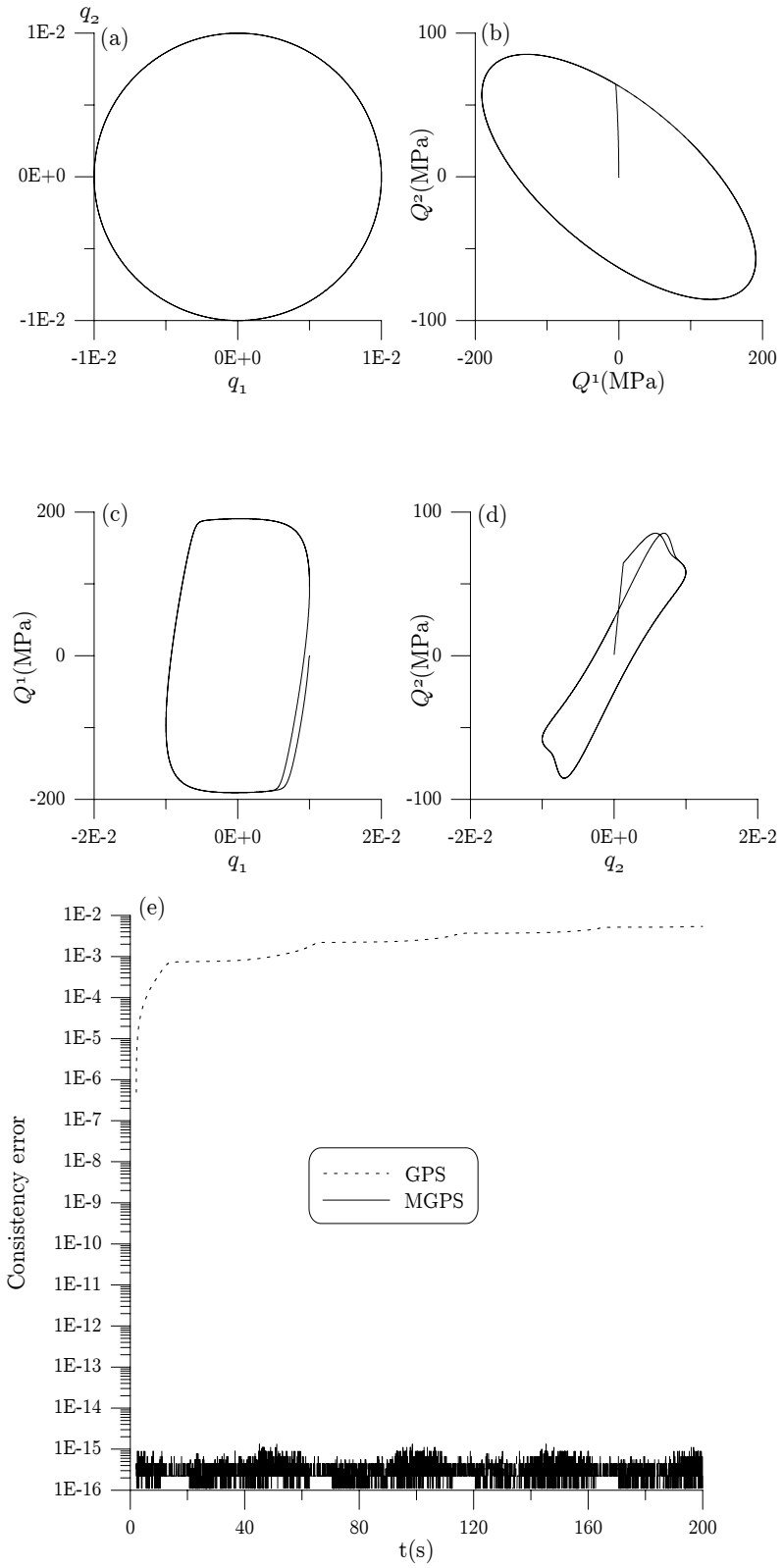

Figure 6 : The responses to a circular strain path in (a), and (b) displaying its corresponding stress path, (c) the cyclic axial stress-axial strain curve, (d) the cyclic shear stress-shear strain curve, and (e) errors in satisfying the consistency condition for GPS and MGPS in Section 5.

from the input strain path in Fig. 5(a). One main feature is that the strain path is closed, but the corresponding stress response has an open path. The other feature is that the strain path is composed of straight lines, but the corresponding stress response has straight-line paths in the elastic phase but elliptical paths in the plastic phase due to yield constraint. In terms of the consistency error defined by $|f-1|$, it is clear that the error by MGPS is far smaller than that by GPS. In all calculations, the time step is fixed to $\Delta t = 0.005$ s.

The model is then subjected to a circular strain path,

$$q_1 = e_0 \cos \omega t, \;\; q_2 = e_0 \sin \omega t, \tag{77}$$

where e_0 and $\omega = 2\pi/T$ are respectively the amplitude and circular frequency of oscillation of the input with T being the period. The input circular strain path was shown in Fig. 6(a) with $e_0 = 0.01$ and $\omega = 2\pi/100$ rad/s. The results include the stress path in Fig. 6(b), hysteresis loops in Figs. 6(c) and 6(d), as well as the errors of consistency condition calculated by the above two schemes in Fig. 6(e). For the non-proportional loading case the consistency errors by GPS increase gradually with time. However, when applied MGPS to this case the consistency errors are depressed largely to the order of 10^{-15}.

7.2 Example two: cubic yield function

As a second example let us consider the following yield condition:

$$\frac{(Q^1)^2}{r_1^2 + 2d_1Q^1 - d_1^2} + \frac{(Q^2)^2}{r_2^2 + 2d_2Q^2 - d_2^2} = 1, \tag{78}$$

where the four material functions r_1, r_2, d_1 and d_2 are used to adjust the shape of yield surface. Since $(Q^1 - d_1)^2 \le r_1^2$ and $(Q^2 - d_2)^2 \le r_2^2$, the terms $r_1^2 + 2d_1Q^1 - d_1^2$ and $r_2^2 + 2d_2Q^2 - d_2^2$ in the above equation can be seen to satisfy

$$r_1^2 + 2d_1Q^1 - d_1^2 > 0, \;\; r_2^2 + 2d_2Q^2 - d_2^2 > 0. \tag{79}$$

The gradient of the yield function is

$$\nabla f = \begin{bmatrix} \frac{2[r_1^2Q^1 + d_1(Q^1)^2 - d_1^2Q^1]}{(r_1^2 + 2d_1Q^1 - d_1^2)^2} \\ \frac{2[r_2^2Q^2 + d_2(Q^2)^2 - d_2^2Q^2]}{(r_2^2 + 2d_2Q^2 - d_2^2)^2} \end{bmatrix}. \tag{80}$$

Substituting Eq. (80) for ∇f into Eq. (64), we obtain $\mathbf{A}_0^s$. Then using the numerical schemes (65) and (67) in Section 6, the responses are calculated. The following parameters: $d_1 = -80$ MPa, $d_2 = -80$ MPa and $r_1 = r_2 = 150$ MPa are used. The results are shown in Fig. 7 with the square strain path and Fig. 8 with the circular strain path. The error tolerance used in solving Eq. (67) is 10^{-8}. It can be seen that the stress paths are located on the yield locus (indicated by dashed line) very well in the plastic phase. In both loading cases the consistency errors by GPS are increased gradually with time. However, when applied MGPS to these loading cases the consistency errors can be depressed to the order in $10^{-12} - 10^{-6}$.

8 Extension to anisotropic elasticity

In this section we extend the numerical solutions of convex plasticity by considering the anisotropic elastic law (8). Substituting Eqs. (6) and (9) into Eq. (8) gives

$$\dot{\mathbf{Q}} + \dot{q}_0 \mathbf{K}\mathbf{n} = \mathbf{K}\dot{\mathbf{q}}. \tag{81}$$

Through some derivations we can obtain the following on-off switching criteria for the mechanism of plasticity:

$$\dot{q}_0 = \frac{\nabla f \cdot (\mathbf{K}\dot{\mathbf{q}})}{\nabla f \cdot (\mathbf{K}\mathbf{n})} > 0 \;\text{ if }\; f = 1 \;\text{ and}$$

$$\nabla f \cdot (\mathbf{K}\dot{\mathbf{q}}) > 0, \tag{82}$$

$$\dot{q}_0 = 0 \;\text{ if }\; f < 1 \;\text{ or }\; \nabla f \cdot (\mathbf{K}\dot{\mathbf{q}}) \le 0. \tag{83}$$

The denominator $\nabla f \cdot (\mathbf{K}\mathbf{n}) = \nabla f \cdot (\mathbf{K}\nabla f)/\|\nabla f\|$ is positive according to the assumptions that $\nabla f \neq \mathbf{0}$ and $\mathbf{K}$ is positive definite.

Eqs. (81), (82) and (83) together yield a two-phase affine nonlinear system:

$$\dot{\mathbf{Q}} = \mathbf{K}\dot{\mathbf{q}} - \frac{\nabla f \cdot (\mathbf{K}\dot{\mathbf{q}})}{\nabla f \cdot (\mathbf{K}\mathbf{n})}\mathbf{K}\mathbf{n} \;\text{ if }\; f = 1 \;\text{ and}$$

$$\nabla f \cdot (\mathbf{K}\dot{\mathbf{q}}) > 0, \tag{84}$$

$$\dot{\mathbf{Q}} = \mathbf{K}\dot{\mathbf{q}} \;\text{ if }\; f < 1 \;\text{ or }\; \nabla f \cdot (\mathbf{K}\dot{\mathbf{q}}) \le 0. \tag{85}$$

Obviously, Eq. (85) is simple to integrate and we only need to consider the numerical integration of Eq. (84), from which the differential equation for the magnitude of $\mathbf{Q}$ can be arranged to

$$\frac{d}{dt}\|\mathbf{Q}\| = \frac{1}{\|\mathbf{Q}\|}\left[\mathbf{Q} \cdot (\mathbf{K}\dot{\mathbf{q}}) - \frac{\nabla f \cdot (\mathbf{K}\dot{\mathbf{q}})}{\nabla f \cdot (\mathbf{K}\mathbf{n})}\mathbf{Q} \cdot (\mathbf{K}\mathbf{n})\right]. \tag{86}$$

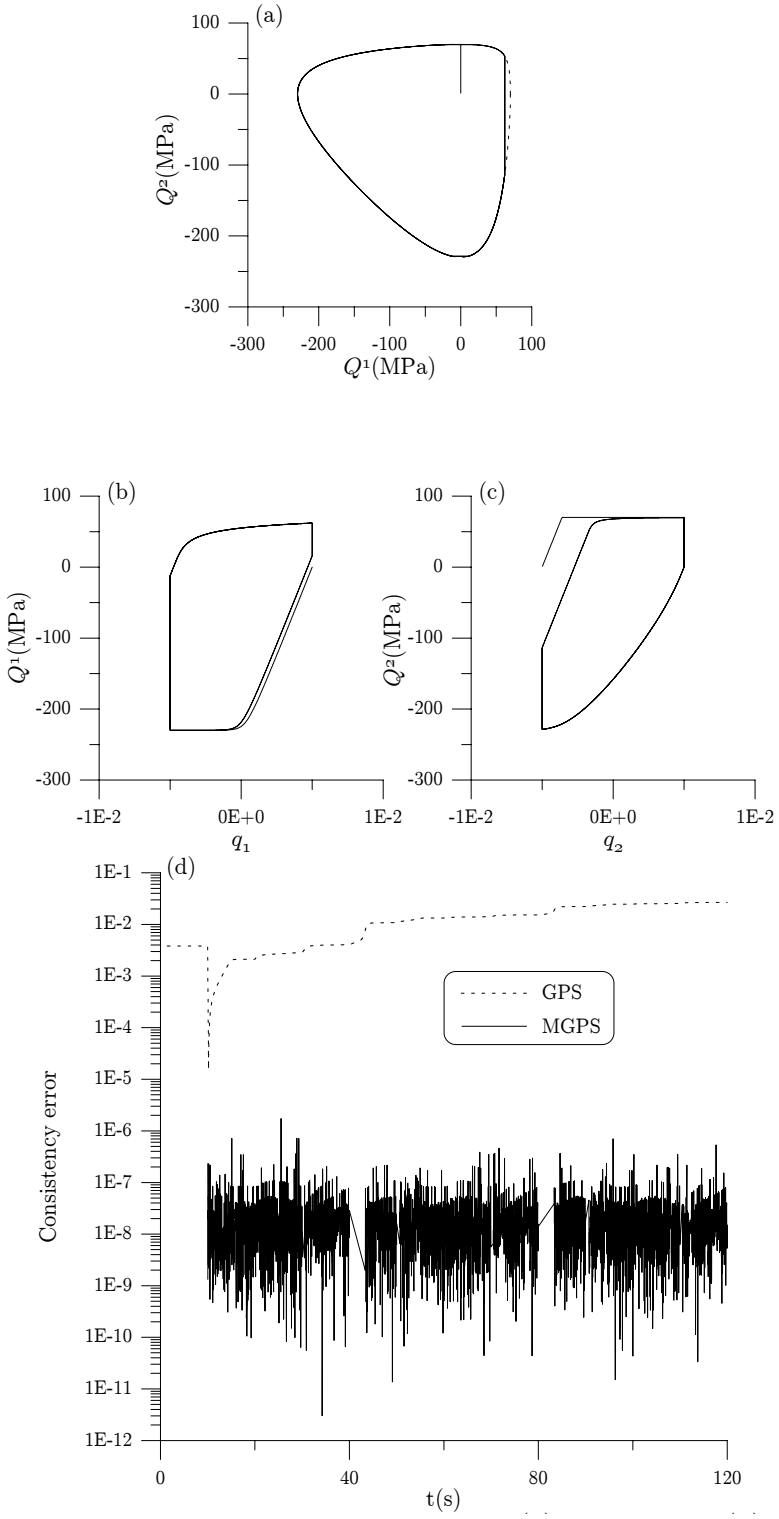

Figure 7 : The responses to a square strain path: (a) stress path, (b) the cyclic axial stress-axial strain curve, (c) the cyclic shear stress-shear strain curve, and (d) errors in satisfying the consistency condition for GPS and MGPS in Section 6.

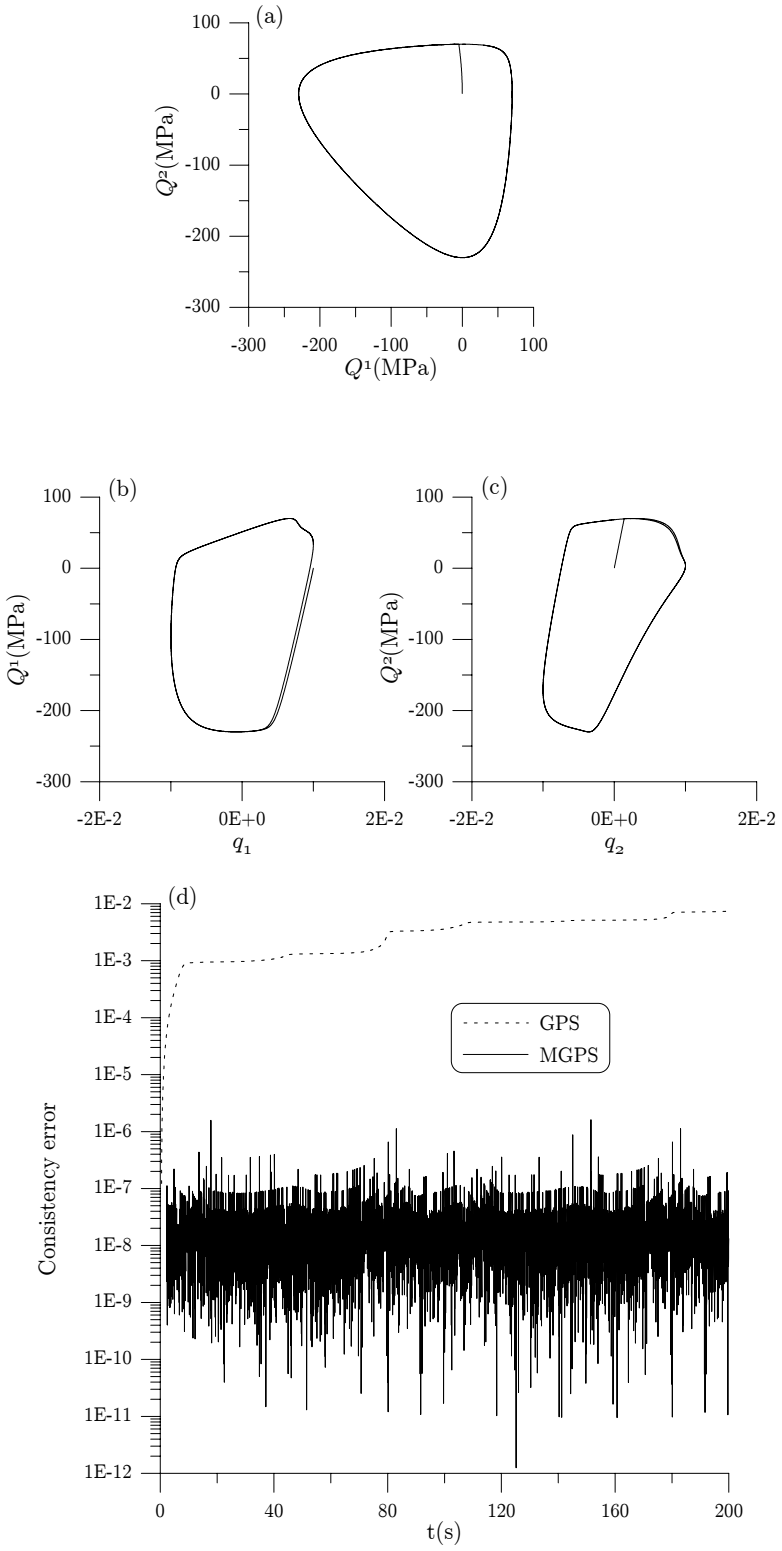

Figure 8 : The responses to a circular strain path: (a) stress path, (b) the cyclic axial stress-axial strain curve, (c) the cyclic shear stress-shear strain curve, and (d) errors in satisfying the consistency condition for GPS and MGPS in Section 6.

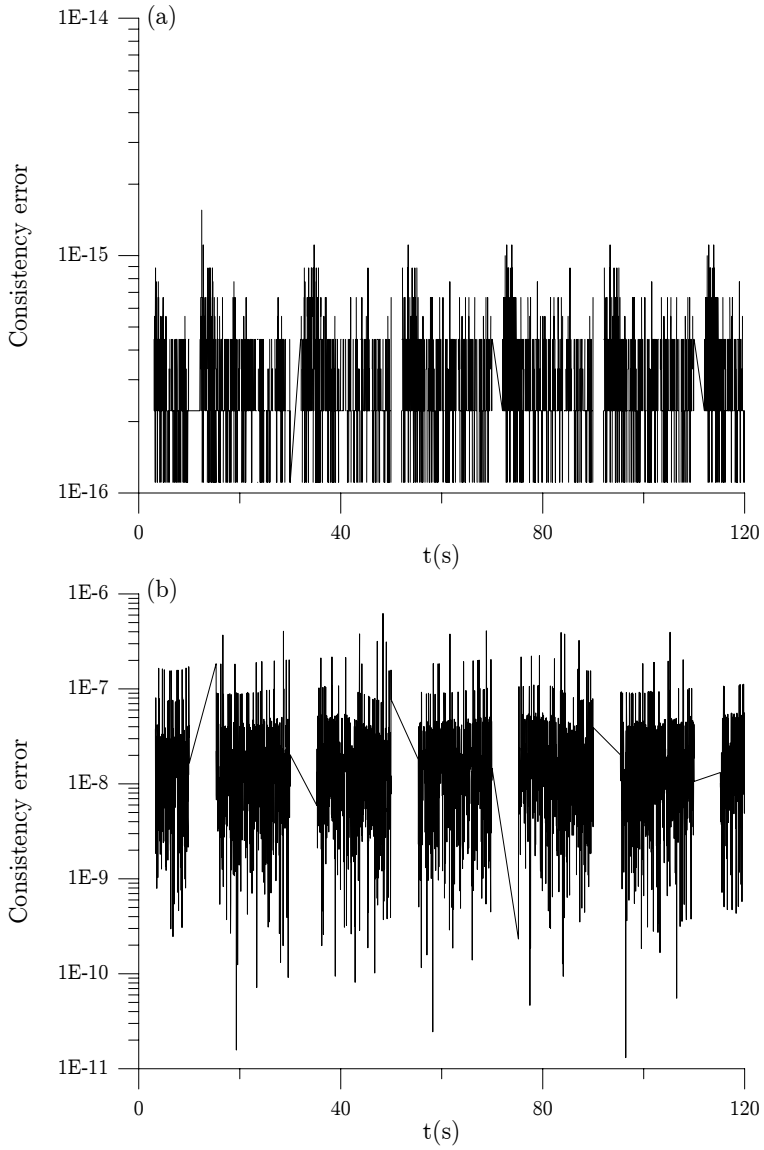

Figure 9 : The errors in satisfying the consistency condition for MGPS in Section 8: (a) example one under square strain path, and (b) example two under square strain path.

The above technique was first developed by Liu (2001) for the general dynamical systems to embed them into an augmented Minkowski space and then derived the group-preserving scheme. In terms of augmented state variables defined by Eq. (62), Eqs. (84) and (86) can be combined together to a quasilinear system (63), where $\mathbf{A}$ is still defined by Eq. (64) but with

$$\mathbf{A}_0^s(\mathbf{Q},t)=\frac{1}{\|\mathbf{Q}\|}\left[\mathbf{K}\dot{\mathbf{q}}-\frac{\nabla f\cdot(\mathbf{K}\dot{\mathbf{q}})}{\nabla f\cdot(\mathbf{K}\mathbf{n})}\mathbf{K}\mathbf{n}\right]. \tag{87}$$

Therefore the modified group-preserving scheme (MGPS) developed in Section 6 is still applicable for this case but with a more complex $\mathbf{A}_0^s$. With the above numerical scheme we compute the two examples in Section 7 again, keeping all parameters unchanged but changing the elastic constants to $K_{11}=5\times10^4$ MPa, $K_{12}=2\times10^4$ MPa and $K_{22}=1.4\times10^4$ MPa to take the elastic anisotropy into account. The consistency errors as shown in Fig. 9 are very small.

9 Conclusions

In this paper we have investigated the convex plasticity equation from several theoretical aspects. By viewing

the plasticity equations as an affine nonlinear dynamical system on the yield manifold, we have proved that there exists a dissipative metric, projecting by it the plastic equation having an elastic type relation in terms of the covariant derivatives of stress and strain. In terms of the Gaussian unit vector and Weingarten map, we presented a quasilinear system of the plastic equation in the space $(\nabla f, \|\nabla f\|)$. Then, we have investigated the internal symmetry group inherent in the plasticity equation, of which the projective proper orthochronous Lorentz group $PSO_o(n,1)$ was found to be an underlying symmetry group. According to the two different representations in spaces $(\nabla f, \|\nabla f\|)$ and $(\mathbf{Q}, \|\mathbf{Q}\|)$, we have developed yield contraint preserving schemes by taking the group properties into account and also using a post-projection method to enforce stress point locating on the yield surface. The newly developed schemes through some numerical examples tests are shown to be stable, efficient, and accurate, and hence can be used in the computations of engineering problems.

Acknowledgement: The financial support provided by the National Science Council of Taiwan under the Grants NSC 92-2212-E-019-006 and NSC 93-2212-E-019-008 is gratefully acknowledged. Acknowledged is also reviewers' comments for improving this paper.

References

Atluri, S. N. (1984): On constitutive relations at finite strain: hypo-elasticity and elasto-plasticity with isotropic or kinematic hardening. *Comp. Meth. Appl. Mech. Engng.*, vol. 43, pp. 137-171.

Atluri, S. N. (1986): An endochronic approach and other topics in small and finite deformation plasticity. In *Finite Elements in Nonlinear Mechanics*, P. Bergan, E. Stein, W. Wunderlich, Eds. pp.17-48, Springer, New York.

Auricchio, F.; Beirão da Veiga, L. B. (2003): On a new integration scheme for von-Mises plasticity with linear hardening. *Int. J. Numer. Meth. Engng.*, vol. 56, pp. 1375-1396.

Chen, J.; Yuan, H.; Wittmann, F. H. (2002): Computational simulations of micro-indentation tests using gradient plasticity. *CMES: Computer Modeling in Engineering & Sciences*, vol. 3, pp. 743-754.

Chen, W. F.; Han, D. J. (1988): *Plasticity for Structural Engineers*. Springer-Verlag, New York.

Hong, H.-K.; Liu, C.-S. (1997): Prandtl-Reuss elastoplasticity: on-off switch and superposition formulae. *Int. J. Solids Struct.*, vol. 34, pp. 4281-4304.

Hong, H.-K.; Liu, C.-S. (1998): On behavior of perfect elastoplasticity under rectilinear paths. *Int. J. Solids Struct.*, vol. 35, pp. 3539-3571.

Hong, H.-K.; Liu, C.-S. (1999a): Internal symmetry in bilinear elastoplasticity. *Int. J. Non-Linear Mech.*, vol. 34, pp. 279-288.

Hong, H.-K.; Liu, C.-S. (1999b): Lorentz group $SO_o(5,1)$ for perfect elastoplasticity with large deformation and a consistency numerical scheme. *Int. J. Non-Linear Mech.*, vol. 34, pp. 1113-1130.

Hong, H.-K.; Liu, C.-S. (2000): Internal symmetry in the constitutive model of perfect elastoplasticity. *Int. J. Non-Linear Mech.*, vol. 35, pp. 447-466.

Im, S.; Atluri, S. N. (1987): A study of two finite strain plasticity models: an internal time theory using Mandel's director concept and a combined isotropic-kinematic hardening theory. *Int. J. Plasticity*, vol. 3, pp. 163-191.

Krieg, R. D.; Krieg, D. B. (1977): Accuracies of numerical solution methods for the elastic-perfectly plastic model. *J. Press. Vess. Tech., ASME*, vol. 99, pp. 510-515.

Lee, E. H.; Liu, D. T. (1967): Finite-strain elastic-plastic theory particularly for plane-wave analysis. *J. Appl. Phys.*, vol. 38, pp. 19-27.

Lee, E. H. (1969): Elastic-plastic deformation at finite strains. *J. Appl. Mech., ASME*, vol. 36, pp. 1-6.

Lee, E. H. (1981): Some comments on elastic-plastic analysis. *Int. J. Solids Struct.*, vol. 17, pp. 859-872.

Liu, C.-S. (2000): A Jordan algebra and dynamic system with associator as vector field. *Int. J. Non-Linear Mech.*, vol. 35, pp. 421-429.

Liu, C.-S. (2001): Cone of non-linear dynamical system and group preserving schemes. *Int. J. Non-Linear Mech.*, vol. 36, pp. 1047-1068.

Liu, C.-S. (2002): Nonlinear Lorentzian and Hamiltonian formulations and their relations. *Int. J. Appl. Math.*, vol. 10, pp. 59-97.

Liu, C.-S. (2003): Symmetry groups and the pseudo-Riemann spacetimes for mixed-hardening elastoplasticity. *Int. J. Solids Struct.*, vol. 40, pp. 251-269.

Liu, C.-S. (2004a): Internal symmetry groups for the Drucker-Prager material model of plasticity and numerical integrating methods. *Int. J. Solids Struct.*, vol. 41, pp. 3771-3791.

Liu, C.-S. (2004b): Lie symmetries of finite strain elastic-perfectly plastic models and exactly consistent schemes for numerical integrations. *Int. J. Solids Struct.*, vol. 41, pp. 1823-1853.

Liu, C.-S. (2004c): A consistent numerical scheme for the von Mises mixed-hardening constitutive equations. *Int. J. Plasticity*, vol. 20, pp. 663-704.

Liu, C.-S.; Hong, H.-K. (2001): Using comparison theorem to compare corotational stress rates in the model of perfect elastoplasticity. *Int. J. Solids Struct.*, vol. 38, pp. 2969-2987.

Mandel, J. (1971): *Plasticité Classique et Viscoplasticité.* Courses and Lectures, No.97, International Centre for Mechanical Sciences, Udine, Springer, New York.

Mukherjee, S.; Liu, C.-S. (2003): Computational isotropic-workhardening rate-independent elastoplasticity. *J. Appl. Mech., ASME*, vol. 70, pp. 644-648.

Nemat-Nasser, S. (1979): Decomposition of strain measures and their rates in finite deformation elastoplasticity. *Int. J. Solids Struct.*, vol. 15, pp. 155-166.

Nemat-Nasser, S. (1982): On finite deformation elastoplasticity. *Int. J. Solids Struct.*, vol. 18, pp. 857-872.

Nemat-Nasser, S. (1991): Rate-independent finite-deformation elastoplasticity: a new explicit constitutive algorithm. *Mech. Mater.*, vol. 11, pp. 235-249.

Ortiz, M.; Popov, E. P. (1985): Accuracy and stability of integration algorithms for elastoplastic constitutive relations. *Int. J. Numer. Meth. Engng.*, vol. 21, pp. 1561-1567.

Sainsot, P.; Jacq, C.; N'elias, D. (2002): A numerical model for elastoplastic rough contact. *CMES: Computer Modeling in Engineering & Sciences*, vol. 3, pp. 497-506.

Schreyer, H. L.; Kulak, R. F.; Kramer, J. M. (1979): Accurate numerical solutions for elastic-plastic models. *J. Press. Vess. Tech., ASME*, vol. 101, pp. 226-234.

Simo, J. C.; Taylor, R. L. (1985): Consistent tangent operators for rate-independent elastoplasticity. *Comp. Meth. Appl. Mech. Engng.*, vol. 48, pp. 101-118.

Thorpe, J. A. (1979): *Elementary Topics in Differential Geometry*. Springer-Verlag, New York.

Wang, L. H.; Atluri, S. N. (1994): An analysis of an explicit algorithm and the radial return algorithm, and a proposed modification, in finite plasticity. *Comp. Mech.*, vol. 13, pp. 380-389.

Xiao, H.; Bruhns, O. T.; Meyers, A. (1999): Existence and uniqueness of the integrable-exactly hypoelastic equation $\overset{\circ}{\tau}^{\star} = \lambda(\mathrm{tr}\mathbf{D})\mathbf{I} + 2\mu\mathbf{D}$ and its significance to finite inelasticity. *Acta Mech.*, vol. 138, pp. 31-50.